2014-08-12

The bone-specific Runx2-P1 promoter displays conserved three-dimensional chromatin structure with the syntenic Supt3h promoter

Rasim Barutcu
University of Massachusetts Medical School

Et al.

10360–10372 *Nucleic Acids Research, 2014, Vol. 42, No. 16*
doi: 10.1093/nar/gku712

The bone-specific *Runx2-P1* promoter displays conserved three-dimensional chromatin structure with the syntenic *Supt3h* promoter

A. Rasim Barutcu[1], Phillip W. L. Tai[1,2], Hai Wu[1,2], Jonathan A. R. Gordon[1,2], Troy W. Whitfield[1,3], Jason R. Dobson[1], Anthony N. Imbalzano[1], Jane B. Lian[1,2], André J. van Wijnen[1], Janet L. Stein[1,2] and Gary S. Stein[1,2,*]

[1]Department of Cell and Developmental Biology, University of Massachusetts Medical School, 55 Lake Avenue North, Worcester, MA 01655, USA, [2]Department of Biochemistry and Vermont Cancer Center, University of Vermont College of Medicine, 89 Beaumont Avenue, Burlington, VT 05405, USA and [3]Program in Bioinformatics and Integrative Biology, University of Massachusetts Medical School, 55 Lake Avenue North, Worcester, MA 01655, USA

Received April 11, 2014; Revised July 04, 2014; Accepted July 22, 2014

ABSTRACT

Three-dimensional organization of chromatin is fundamental for transcriptional regulation. Tissue-specific transcriptional programs are orchestrated by transcription factors and epigenetic regulators. The RUNX2 transcription factor is required for differentiation of precursor cells into mature osteoblasts. Although organization and control of the bone-specific *Runx2-P1* promoter have been studied extensively, long-range regulation has not been explored. In this study, we investigated higher-order organization of the *Runx2-P1* promoter during osteoblast differentiation. Mining the ENCODE database revealed interactions between *Runx2-P1* and *Supt3h* promoters in several non-mesenchymal human cell lines. *Supt3h* is a ubiquitously expressed gene located within the first intron of *Runx2*. These two genes show shared synteny across species from humans to sponges. Chromosome conformation capture analysis in the murine pre-osteoblastic MC3T3-E1 cell line revealed increased contact frequency between *Runx2-P1* and *Supt3h* promoters during differentiation. This increase was accompanied by enhanced DNaseI hypersensitivity along with RUNX2 and CTCF binding at the *Supt3h* promoter. Furthermore, interplasmid-3C and luciferase reporter assays showed that the *Supt3h* promoter can modulate *Runx2-P1* activity via direct association. Taken together, our data demonstrate physical proximity between *Runx2-P1* and *Supt3h* promoters, consistent with their syntenic nature. Importantly, we identify the *Supt3h* promoter as a potential regulator of the bone-specific *Runx2-P1 promoter*.

INTRODUCTION

The Runt-related transcription factor 2 (RUNX2/CBFα1/AML3) is essential for osteoblastic differentiation and is required for bone and cartilage development (1–5). A complete knockout of *Runx2* leads to embryonic lethality marked by an absence of bone development and ossification (2,6,7). Moreover, RUNX2 interacts with the nuclear matrix to affect histone modifications and chromatin remodeling (8–10).

The murine *Runx2* gene is located on chromosome 17 and spans a region of ∼210 kb. Two predominant *runx2* RNAs are transcribed from distinct promoters. The *runx2 type-II* transcript controlled by the *P1* promoter is exclusively expressed in osteo-progenitor cells and is stimulated upon bone formation. The *runx2 type-I* transcript is driven by the *P2* promoter and is expressed in both osteogenic and non-osteogenic mesenchymal tissues (11). During embryonic development, *P1* promoter driven *runx2 type-II* is the major transcript expressed in the developing skeleton (12). Consistent with this pattern, the specific loss of expression from the *Runx2-P1* promoter in mice results in severe developmental defects with cleidocranial dysplasia (CCD)-like symptoms (12).

*To whom correspondence should be addressed. Tel: +1 802 656 4874; Fax: +1 802 656 2140; Email: gary.stein@uvm.edu
Present addresses:
Jason R. Dobson, Center for Computational Molecular Biology, Department of Computer Science, Brown University, 115 Waterman Street, Providence, RI 02906, USA
André J. van Wijnen, Department of Biochemistry and Molecular Biology, Mayo Clinic, 200 First Street SW, Rochester, MN 55905, USA

Runx2 displays a syntenic relationship with the suppressor of Ty3 homolog (*Supt3h*) gene, whose promoter resides within the first intron and ∼38 kb downstream of the *Runx2-P1* transcriptional start site (TSS). SUPT3H is a TBP-associated factors (TAF)-associated protein that is a component of the human histone acetyl transferase STAGA complex (SPT3-TAF9-GCN5-acetylase) (13–16). These two genes have different expression profiles; *Runx2-P1* is developmentally regulated, while *Supt3h* is ubiquitously expressed and is essential in all tissues. Interestingly, the syntenic relationship between *Runx2* and *Supt3h* is conserved among species from humans to sponges (17), which suggests the existence of an evolutionarily conserved selective pressure to preserve this syntenic relationship. This pressure may be due to a shared or linked regulatory control mechanism and a potential for crosstalk between these two genes (18,19).

In this study, we investigated the higher-order organization of the *Runx2* locus in several cell types. Mining the ENCODE database through the WashU Epigenome Browser (20), we identified long-range associations between the *Runx2-P1* and *Supt3h* promoter regions. Carrying out chromosome conformation capture (3C) analyses in RAW 264.7 murine macrophage cells, where *Runx2-P1* is silent, we confirmed the existence of this interaction. As *Runx2-P1* activity is increased during osteoblastogenesis, we next asked whether this interaction is dynamic and functional. Interestingly, 3C analyses revealed an increase in the interaction frequency between the *Runx2-P1* and *Supt3h* promoters in MC3T3-E1 murine pre-osteoblast cultures throughout osteoblastic differentiation. The *Supt3h* promoter also showed enrichment for DNaseI hypersensitivity (DHS) and CCCTC-binding factor (CTCF) and RUNX2 localization with the onset of osteogenesis. Finally, we provide evidence that the *Supt3h* promoter can interact with *Runx2-P1 in-trans* and modulate its expression in a differentiation-dependent manner.

MATERIALS AND METHODS

WASHU epigenome and UCSC genome browser search

Online interaction data were obtained from the WASHU epigenome browser (20) and the UCSC Genome Browser (21). IMR90 HiC data (22) and the PolII ChIA-PET data (23) were extracted for the hg19:chr6:45 250 000–45 370 000 genomic coordinates. The DHS tracks were obtained for University of Washington (UW) tracks for MCF7 and K562, and from Duke University tracks for IMR90. The MCF7 CTCF ChIP-seq data were extracted from UW generated tracks. Both CTCF and PolII tracks were obtained from Stanford/Yale/Duke/Harvard tracks for K562 and IMR90 cells. The MCF7 PolII ChIP-seq data were obtained from UT Austin tracks. All RNA-seq data were gathered from the Cold Spring Harbor Laboratory ENCODE tracks.

Cell culture

The MC3T3-E1 clone-4 pre-osteoblastic murine cell line (24) was obtained from the American Type Culture Collection (ATCC, Manassas, VA). Growth-phase cultures were maintained in α-MEM without ascorbic acid (Hyclone, Thermo Fisher Scientific, Rochester, NY) and supplemented with 1% penicillin-streptomycin (Gibco, Life Technologies, Grand Island, NY), 2 mM L-glutamine (Gibco, Life Technologies, Grand Island, NY) and 10% fetal bovine serum (Hyclone, Thermo Fisher Scientific, Rochester, NY). When cultures reached ∼90% confluency, differentiation was initiated by the addition of 142 μM ascorbic acid (Sigma-Aldrich, St Louis, MO). After 2 days, the ascorbic acid concentration was increased to 280 μM and 5 mM β-glycerophosphate (Sigma-Aldrich, St Louis, MO) was added. Cultures were maintained at 37°C and at 5% CO_2.

Chromosome conformation capture (3C)

3C assays were performed as previously described (25,26), with the following modifications: 3C restriction fragments were defined by BglII enzyme digestion. The anchor fragment used to query *Runx2-P1* chromosomal interaction spans from −975 to +1113 (mm9 chr17: 44 950 469–44 952 567). ∼1 × 10^8 MC3T3-E1 cells were fixed with 1% formaldehyde in serum free α-MEM for 10 min at room temperature. Formaldehyde was quenched by the addition of 0.125 M glycine. Nuclei were released by Dounce homogenization in ice-cold lysis buffer (10 mM Tris-HCl pH 8.0, 10 mM NaCl, 0.2% NP-40) containing cOmplete, Mini Protease Inhibitor Cocktail (Roche Applied Science, Indianapolis, IN). Nuclei were collected and subjected to overnight digestion with 400 U of BglII (New England BioLabs, Ipswich, MA). The enzyme reaction was halted by incubation at 65°C for 30 min in the presence of 10% sodium dodecyl sulphate. Samples were aliquoted into 22 separate tubes and were diluted 40-fold in ligation buffer (25) and subjected to proximity-mediated ligation with 10 U of T4 DNA Ligase (Invitrogen, Life Technologies, Grand Island, NY) per reaction for 4 h at 16°C. Nuclear material was reverse cross-linked by overnight incubation with Proteinase K at 65°C. Ligated chromatin was extracted by phenol-chloroform extraction followed by ethanol precipitation. 3C primers that span the *Runx2* gene locus were designed by Primer3 software and are listed in Supplementary Table S1. The annealing temperatures of all 3C primers were 60 ± 1°C. The polymerase chain reaction (PCR) conditions were 95°C for 8 min followed by 35 cycles of 95°C for 30 s, 60°C for 30 s and 72°C for 30 s, followed by 72°C for 8 min. All 3C PCR products were analyzed on 1% agarose gels stained with ethidium bromide. Gel quantifications were analyzed using the GEL-QUANT software (www.gelquant.org).

Interaction frequencies were determined by assessing fold-change of 3C PCR amplification product of sample chromatin compared to randomly ligated BglII digested bacterial artificial chromosomes (BACs) that span the *Runx2* locus. The following BAC clones, which span the *Runx2-Supt3h* locus and a gene desert region, were used: BACPAC CHORI (Children's Hospital Oakland Research Institute) catalog numbers RP23-22H7, RP23-92H18, RP23-356F5, RP23-443F11, and RP23-238O6. The ligation efficiencies of all 3C samples were normalized to each other by taking the $\log_2$ average of the ligation frequencies of a gene desert region (27) for samples generated with BglII, and ERCC3 locus for samples generated with HindIII. The BAC control template was prepared by

mixing the different BACs in equimolar concentrations, followed by digestion and ligation. Then, the interaction frequency was calculated by dividing the amount of PCR product from the 3C template by the amount of PCR product from the BAC control template, thereby normalizing for differences in primer efficiencies. All of the 3C primer pairs yielded similar amounts of product with both the 3C and the BAC templates. Primers that gave very low PCR yields were discarded. 3C data represent the averaged ligation frequencies of two independent cultures quantified in three separate library preparations. Student's *t*-test was used to assess the *P* values.

DNase-seq

Genome-wide DNase-hypersensitivity mapping of osteoblast cultures was performed by adapting the DNase-seq protocol from Song *et al.* (28) with slight modifications. Approximately 40×10^6 growth-phase (day 0 or d0) or matrix-deposition stage (day 9 or d9) MC3T3-E1 cells were harvested and were each subjected to 4, 12 and 40 U/μl of DNaseI for 15 min at 37°C. Steps involving the isolation of chromatin embedded in agarose included a treatment with 10 U/ml β-agarase for 2 h at 37°C before extracting with phenol:chloroform:isoamyl alcohol (25:24:1 v/v) and ethanol precipitation. Peak signals in this report represent a single biological sample for each culture condition sequenced twice (combined technical duplicates) and normalized using align2rawsignal (A. Kundaje, http://code.google.com/p/align2rawsignal/). DNase-seq analysis was validated by 4-fold representation (two biological replicates, each with technical duplicates) that passes ENCODE Consortium standards on F-seq called peaks (29) using IDR analysis (data not shown; (40)). The DNase-seq data were deposited under the accession GSE55046.

Reverse-transcriptase qPCR

Total RNA from cultures was extracted using TRIzol reagent (Invitrogen, Life Technologies, Grand Island, NY) followed by DNase treatment with DNA-Free RNA Kit (Zymo Research, Irvine, CA) according to manufacturer's instruction. cDNA was prepared using the SuperScriptIII First-Strand Synthesis System (Invitrogen, Life Technologies, Grand Island, NY). qPCR was performed with the iTaq SYBR Green Supermix with ROX (Bio-Rad, Hercules, CA) and on the 7300 Sequence Detection System (Bio-Rad Laboratories, Hercules, CA). Relative transcript levels were determined by the ΔΔCt method and normalized to *gapdh*. Primer sequences for *runx2P1, runx2P2, osteocalcin, bone sialoprotein and gapdh* are described elsewhere (12). Primers for detection of *supt3h* message were designed using FoxPrimer (www.foxprimer.org; Dobson *et al.*, manuscript in preparation) and are: forward, 5′-AAGGCATTGACGAGGATGAC-3′ and reverse, 5′-TCTTCAAACATTGCCAGCAG-3′. Student's *t*-test was used to assess the *P* values.

Reporter constructs

The design and preparation of the 3-kb (−2821 to −16) and 0.6-kb (−629 to −16) luciferase constructs are described elsewhere (30). The *Runx2-P1* 0.9-kb Luc construct was derived from the 3-kb luciferase construct by deleting sequence between −2821 and −966 using the quick-change method for large fragment deletion (30). The murine 3.3-kb *Supt3h* promoter region (3315 bp) was PCR cloned from mouse C57BL/6 genomic DNA using Phusion High-Fidelity DNA Polymerase using the following forward and reverse primers: 5′-GCTCGCACTCAGCTTTGGGCA-3′ and 5′-GGGAGAGACAGGCAAGGAGGGG-3′. The 3.3-kb *Supt3h* promoter region flanked by KpnI restriction sites was cloned upstream of 0.9-kb *Runx2-P1* pGL3 luciferase vector (GENEWIZ, Inc., South Plainfield, NJ). To generate the *Supt3h*-TOPO construct, the 3.3-kb *Supt3h* promoter region was subcloned into the pCR-4Blunt-TOPO vector using the Zero Blunt TOPO PCR Cloning Kit following manufacturers' recommended conditions. The *Supt3h*-DHS1 and *Supt3h*-DHS2 TOPO and 0.9-kb pGL3 constructs described here were generated by similar methods using the following primer sets:

Supt3h-DHS1:FW, 5′-GGA ACT TTG TAG AAA GGA ACG GGG G-3′,RV,5′-CAT GCG CAC CCG GCT GGC C-3′; *Supt3h*-DHS2:FW, 5′-CGC TCT CGC CGC ACG GC-3′,
RV, 5′-CTC CCA TAA ACC TGA GTT TTG AGC TAG G-3′; *Supt3h*-0.5 kb: FW, 5′-GAT ATT AGT TGA GCA GAA TTT TAA T-3′, RV, 5′-TAC TTC ATT AAT GTC TTG CCT ATG-3′
Supt3h-0.6 kb:FW, 5′-TAA CTT CAC AAG AGC TTC GTT TTC-3′, RV 5′ TAA ACA AAC AAA CAA ACA AAC TGC T-3′; *Supt3h*-1.1 kb:FW 5′TAA CTT CAC AAG AGC TTC GTT TTC-3′, RV 5′-TAC TTC ATT AAT GTC TTG CCT ATG-3′.

The empty-TOPO construct described in this report was generated by allowing the pCR-4Blunt-TOPO vector to self-circularize, a low-frequency event that occurs when reactions lack a blunt-ended fragment. The *TK*-pGL3 and SV40-renilla constructs were kind gifts from Dr Stephen D. Hauschka.

Co-transfections and Luciferase reporter assays

Growth-phase MC3T3-E1 clone-4 cells were grown to >90% confluency and co-transfected with Firefly Luciferase test constructs and SV40-Renilla constructs using Lipofectamine (Invitrogen, Life Technologies, Grand Island, NY) and Plus Reagent (Invitrogen, Life Technologies, Grand Island, NY) according to manufacturer's instructions. 2.5 μg of total plasmid DNA was transfected per 60 mm plate as described in the Results section. At designated days post-switch, cultures were harvested and reporter activities were measured using the Dual-Luciferase Reporter Assay System (Promega, Madison, WI) on a VICTOR X4 Multilabel Plate Reader (Perkin Elmer, Waltham, MA) according to manufacturers' instructions. Each test condition described is represented by at least nine replicate plates, and statistical significance values are reported where applicable.

Interplasmid 3C

We adapted a 3C-qPCR (31) approach for analyzing the interaction frequency between two transiently co-transfected plasmid constructs. We have named this method interplasmid 3C (i3C). The following primers were designed to span *SphI* restriction sites: TOPO 5′-GCACGTACTCGGATGGAAG-3′, pGL3 5′-CCGAGTGTAGTAAACATTCCAAAAC-3′, Runx2 internal control FW 5′-CTCTTCATTTGCACTGGGTCACACG-3′ and *Runx2* internal control RV 5′-CCAGGGAAGTGGAGGGAAGGGTTG-3′. qPCR was performed as described above. Enrichment of ligation products was assessed by normalizing the Ct values of the 3C-ligation products to an internal loading control. Relative ligation frequency was obtained by normalizing the enrichment values to the empty TOPO–empty pGL3 control combination. Student's *t*-test was used to assess the *P* values.

RESULTS

Identification of a long-range interaction between the *Runx2-P1* and *Supt3h* promoters

In order to assess the prevalence of long-range looping interactions between *Runx2-P1* and *Supt3h* promoters in a variety of cellular contexts, we examined (using the WashU Epigenome Browser (20)) publicly available HiC and ChIA-PET datasets that are part of the ENCODE project (see the Materials and Methods section). Because DHS and CTCF are strongly correlated with the presence of long-range interactions (32), we decided to include these marks in our analysis. In addition, RNA-seq and PolII ChIP-seq data were included as parameters of transcriptional activity. HiC (high-throughput chromosomal conformation capture) methodology probes long-range chromosomal interactions on a genome-wide scale (33). ChIA-PET (Chromatin Interaction Analysis by Paired-End Tag Sequencing), on the other hand, identifies chromatin interactions at regions associated with a transcription factor or a complex of interest via a combination of chromatin immunoprecipitation (ChIP) and 3C mapping (34).

IMR90 human lung fibroblasts display a long-range interaction between *Runx2-P1* and *Supt3h* promoter regions, which are ∼38 kb away from each other (Figure 1a). Results from individual IMR90 HiC experimental replicate tracks show the same result (Supplementary Figure S1a). Moreover, RNA-seq data suggest that the *Supt3h* gene is transcribed. Consistent with the observation of the chromatin interaction, the *Supt3h* promoter also harbors DHS, CTCF and PolII binding. There is no detectable RNA-seq signal at the *Runx2-P1* promoter region, as expected from a non-osteogenic cell line (Figure 1a).

In K562 leukemia cells, ChIA-PET data for interactions bound by PolII demonstrate many looping interactions within the intervening sequences between *Runx2-P1* and *Supt3h* promoters, as indicated by the different sizes of arcs in Figure 1b. Comparison of data from individual replicates suggests that the variability of detectable interaction events within this region is fairly high (Supplementary Figure S1b). However, the interaction between the *Runx2-P1* and *Supt3h* promoter regions is reproducible between these two replicates (Supplementary Figure S1b). The epigenetics marks correlating with higher-order chromatin organization such as the presence of DHS, enrichment of CTCF and PolII, and a strong RNA-seq peak are all observed in the *Supt3h* region. Similar to the case in IMR90 cells, there is no detectable ChIP-seq or RNA-seq signal in the *Runx2-P1* promoter (Figure 1b). Interestingly, the intensity and locations of the looping interactions in K562 cells greatly differ between the *Runx2* and *Supt3h* promoter regions. This may be due to PolII tracking through the *Supt3h* gene body during active transcription. It is worth noting that the *Supt3h* promoter region also makes long-range interactions with regions other than the *Runx2-P1* promoter, suggesting a complex regulatory interaction network for these genes.

ChIA-PET data for MCF7 PolII also suggest a physical interaction between *Runx2* and *Supt3h* promoter regions, accompanied by a DHS, transcription of the *Supt3h* gene, and PolII and CTCF binding to the *Supt3h* promoter (Figure 1c). There is no transcription detected from the *Runx2-P1* promoter. In comparison with the K562 PolII ChIA-PET data, looping between the *Supt3h* promoter and other regions is observed in addition to many local interactions in MCF7 cells. In this dataset, the interaction between *Runx2-Supt3h* is detected in only one of the two experimental replicates, which might indicate contacts are rare in MCF7 compared to K562 cells.

Because there is a long-range interaction between *Runx2-Supt3h* promoters in human cell lines that lack detectable *Runx2-P1* driven transcription as assessed by RNA-seq tracks, we next asked whether this interaction also exists in a murine cell line where *Runx2* is silent. In order to address this question, we used the 3C approach (25,26) to examine the RAW 264.7 murine macrophage cell line, which exhibits low levels of *Runx2* expression as assessed by RT-qPCR (Supplementary Figure S2).

3C is a widely used method that employs the intramolecular ligation of enzymatically digested cross-linked chromatin. Unique ligation junctions are quantified by PCR to assess the relative proximity of restriction fragments of interest to detect captured interacting chromosomal domains (25,26). We analyzed the interaction profile of the *Runx2-P1* promoter with the BglII restriction fragments encompassing the *Supt3h* and *Runx2-P2* promoters (Figure 1d). The 3C primers were designed to query the ligation frequency between the anchor fragment located at the *P1* promoter and BglII restriction fragments flanking the *Supt3h* and *Runx2-P2* promoter regions (see Supplementary Table S1 for the primer list).

Similar to the cases observed in different human cell lines that have minimal *Runx2* expression (Figure 1a–c), we found long-range interactions between the *Runx2-P1* and *Runx2-P2* regions, and between *Runx2-P1* and the *Supt3h* promoters (Figure 1d).

Taken together, these findings suggest that the *Runx2-P1* and *Supt3h* promoters are in close proximity in four different cell types of human and mouse origin. The human cell lines queried show the presence of DHS, and the enrichment of CTCF and PolII at the *Supt3h* promoter. The presence of DHS and the enrichment of CTCF at this re-

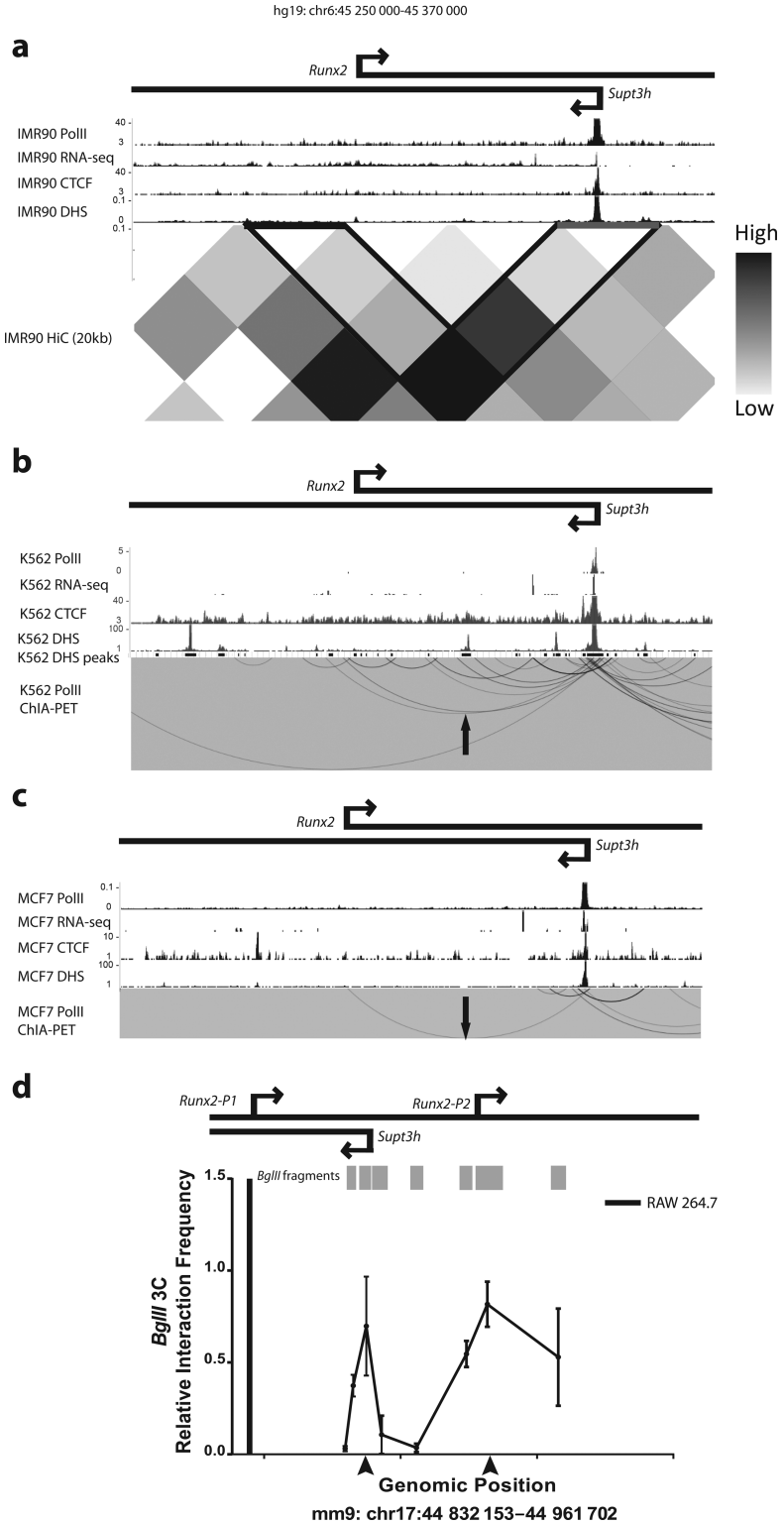

Figure 1. (**a**) WashU Epigenome Browser snapshot of the HiC interaction frequencies in IMR90 cells (22) between the *Runx2-P1* and *Supt3h* promoter regions. The genes are diagramed on top, and the transcriptional start sites are indicated by the arrows. The 20-kb regions encompassing the *Runx2-P1* and *Supt3h* promoters are highlighted with black bars. In the HiC heatmap, darker colors represent higher interaction frequency. UCSC genome browser screenshots of ChIP-seq profiling signal tracks for PolII, CTCF, DHS and RNA-seq data of IMR90 cells are labeled. (**b**, **c**) ChIA-PET interactions bound by PolII within the local *Runx2-P1* and *Supt3h* promoter regions, accompanied by UCSC genome browser screenshot of PolII and CTCF ChIP-seq, DHS and RNA-seq signals for K562 (b) and MCF7 (c) cells. The arrows indicate the specific interaction between *Runx2* and *Supt3h* promoter regions. (**d**) Chromosome conformation capture (3C) analysis of the *Runx2* gene locus in RAW 264.7 macrophages. The x-axis represents the genomic position and the y-axis shows the relative interaction frequency. Anchor *BglII* fragment at *Runx2-P1* is indicated with a black bar. Gray bars indicate the *BglII* restriction fragments. Arrowheads point at the *Supt3h* and *Runx2-P2* interactions. Error bars: S.E.M.

gion correlate with the observation of the long-range interaction (32,35). In the mouse RAW 264.7 macrophage cells, in which the *Runx2* gene is transcriptionally silent, the same interaction is also observed via 3C analysis. These findings suggest that these interactions represent a static three-dimensional structure established between the *Runx2-P1* and *Supt3h* promoters in cells that have minimal levels of *Runx2-P1* driven transcription.

Interaction frequency between *Runx2-P1 and Supt3h* promoters is increased during osteoblast differentiation

Runx2 is fundamental for bone formation and maintenance. Because *Runx2-P1* driven transcription increases during osteogenesis (12,36), we asked whether the long-range association observed between the *Runx2-P1* and *Supt3h* promoters is altered during osteoblast differentiation. We compared the MC3T3-E1 cell line at growth phase, pre-osteoblasts (d0) versus differentiating cultures at matrix-deposition stage (d9), as *Runx2* transcript levels have been shown to increase ∼2–6-fold by the matrix-deposition stage of osteoblastogenesis (37,38). This marked increase in transcription occurs within the first 9 days of differentiation.

Using the 3C methodology, we queried the interaction profile of the *Runx2-P1* promoter with sequences flanking ∼300 kb 5′ and 3′ of this promoter in d0 and d9 cultures. The 3C results show that the *Runx2-P1* anchor fragment displays high-interaction frequency with the fragment encompassing the *Runx2-P2* promoter in both d0 and d9 cultures (Figure 2a). Cells cultured in differentiation conditions for d9 show a modest, statistically insignificant increase in the interaction frequency between the *Runx2-P1* and *Runx2-P2* promoters. A notable interaction between the anchor fragment and the fragment encompassing the *Supt3h* promoter in d0 cultures was also observed. Interestingly, there was a statistically significant ∼2-fold increase ($P < 0.05$) in interaction frequency at this region in d9 versus d0 cultures (Figure 2a). Interaction with the *Supt3h* promoter region was among the most significantly changed throughout the entire 600-kb *Runx2* locus during differentiation, suggesting a mechanistic link with the conserved syntenic nature of these genes.

To confirm the interactions between the *Runx2-P1, Supt3h, and Runx2-P2* promoter regions in differentiating (d9) osteoblasts, we utilized the 3C primer that is most proximal to the *Runx2-P2* promoter as the anchor primer to probe for interactions between the *Runx2-P2* promoter and flanking regions. When the BglII fragment spanning the *Runx2-P2* promoter is used as the anchor, strong interaction frequencies with both *Runx2-P1* and *Supt3h* promoters are observed (Figure 2b).

To further validate these results, we repeated the 3C experiments with an alternative design, using the HindIII restriction enzyme instead of BglII. Interaction frequencies between the anchor *Runx2-P1* fragment and the HindIII fragments at the *Supt3h* promoter region were analyzed in d0 and d9 MC3T3 cells. We observed that the HindIII fragment at the *Supt3h* TSS region has a significantly higher interaction frequency with the *Runx2-P1* promoter in d9 cultures than in d0 cultures (Supplementary Figure S3). It is also worth noting that the looping HindIII and BglII fragments (Figure 2a) at the *Supt3h* promoter overlap with each other. HindIII fragments flanking the BglII fragment showed similar interaction frequencies in d0 and d9 cultures (Supplementary Figure S3).

The increase in chromatin association between the *Runx2-P1* and *Supt3h* promoters during differentiation suggests a possible regulatory relationship between these two regions, while other interaction events appear to remain constant.

Interactions between *Runx2-P1* and *Supt3h* are enriched for CTCF, RUNX2 and DHS during osteoblast differentiation

Genome-wide studies have recently shown that many developmentally regulated genes exhibiting long-range interactions are enriched for CTCF (32,35). Additionally, RUNX2 protein is shown to be a component of the nuclear matrix and to act as a nuclear scaffolding factor (1,9,10). We asked if the local chromatin state is altered at the *Runx2-P1* and *Supt3h* promoter regions during differentiation, in which the looping intensity is significantly increased upon differentiation.

We have recently employed a comparative analysis of the genome-wide enrichments of CTCF and RUNX2 via ChIP-seq during MC3T3-E1 differentiation (38). To determine whether the interactions between the *Runx2-P1* and the *Supt3h* promoter regions correlate with the recruitment of CTCF and/or RUNX2, we extracted the ChIP-seq data encompassing the *Runx2* locus. Additionally, to address whether there is altered nucleosome association at these regions due to a change in factor occupancy, we carried out DNase-seq experiments in differentiating MC3T3 cultures (Figure 3) (40).

Interestingly, the DHS profile of the genomic region surrounding the *Runx2-Supt3h* gene locus shows the most pronounced peak at the *Supt3h* promoter region in both d0 and d9 cultures. ChIP-seq analysis demonstrates that CTCF, which is implicated in mediating long-range interactions, is enriched at the *Supt3h* promoter on d0, consistent with the basal level of interaction in cells that lack *Runx2-P1* activity. As pre-osteoblasts undergo osteoblast differentiation, we also observed a modest increase of CTCF enrichment at the *Supt3h* and *Runx2-P1* promoters (d9), coinciding with a similar increase in the DHS signal at this region (Figure 3). Interestingly, the timing of enrichment of CTCF at the *Supt3h* promoter overlaps with the increased looping frequency with *Runx2-P1* (Figure 2a). Moreover, ChIP-seq data demonstrate that RUNX2 enrichment is substantially increased at the *Runx2-P1, Runx2-P2* and *Supt3h* promoters upon differentiation (Figure 3).

The increase of DHS and CTCF enrichment at the *Supt3h* promoter, together with the differentiation-dependent increased looping frequency, suggests a mechanistic link between the *Supt3h* and *Runx2-P1* promoters. The enrichment of RUNX2 observed at both *Runx2-P1* and *Supt3h* promoters is correlated with the increase in transcriptional activity of the bone-related *Runx2-P1* promoter (12), implying a regulatory role for sequences within the *Supt3h* promoter.

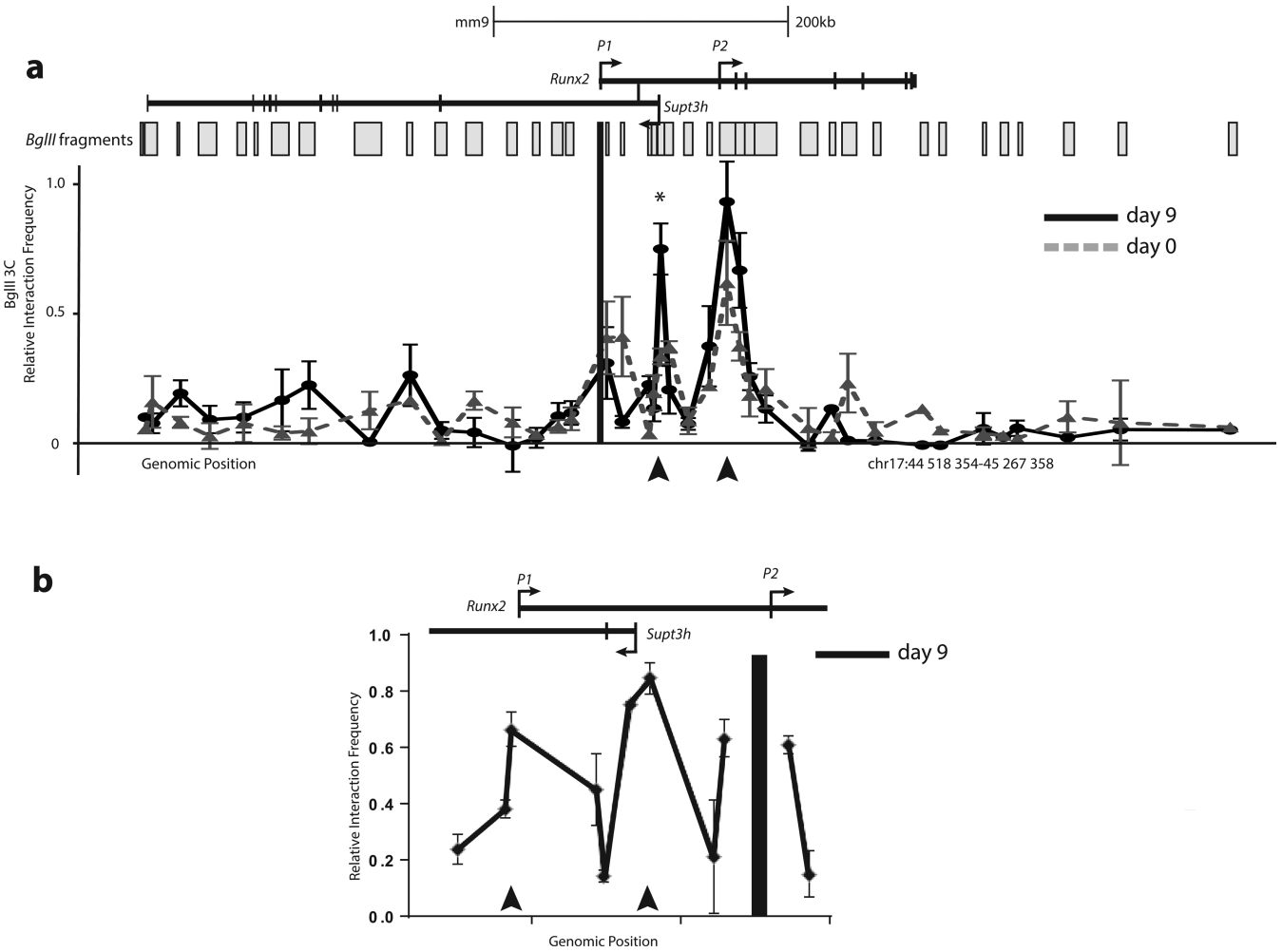

Figure 2. 3C analysis of *Runx2-P1* promoter. (**a**) 3C analysis of the *Runx2* locus in proliferating (d0 and d9) post-differentiation MC3T3-E1 cultures. The genes are diagramed on top, and the TSSs are designated by the arrows whereas the exons are represented by black bars. The anchor fragment is designated by a black bar at *Runx2*-P1. The x-axis represents the genomic position and the y-axis shows the relative 3C interaction frequency. The highest interaction frequency value (d9, *Runx2-P2* peak) was normalized to 1. Error bars: S.E.M. (**b**) 3C analysis of d9 MC3T3 cultures with the anchor fragment located on *Runx2-P2*. The black arrows point at *Runx2-P1* and *Supt3h* regions. Error bars: S.E.M. (*$P < 0.05$ by Student's *t*-test).

Supt3h expression levels remain constant during osteoblast differentiation

As the *Supt3h* promoter region undergoes alterations in chromatin conformation, DHS and factor binding profiles, we analyzed the expression of *Supt3h* throughout several time points during osteoblast differentiation. As expected (39), transcript levels of *Runx2-P1* and *Runx2-P2* increased between d0 and d9 cultures (2.5-fold and 1.6-fold, respectively) (Figure 4a). mRNA levels of bone-sialoprotein (*ibsp*) and osteocalcin (*bgalp2*), markers for osteoblast differentiation, were increased several-fold between the same two time points (Figure 4a) while the *supt3h* mRNA levels were relatively unchanged. In order to rule out the possibility that *supt3h* mRNA levels might fluctuate between d0 and d9, we measured the *supt3h* expression levels at additional time points during differentiation. Cultures harvested between d2 and d7 after initiation of differentiation showed no significant changes in *supt3h* RNA levels (Figure 4b). This lack of change in RNA levels is also true of cultures undergoing mineralization for 28d post-differentiation (data not shown). Therefore, despite changes in the local chromatin architecture of its promoter (Figures 2a and 3), *supt3h* expression was not changed during osteoblastic differentiation.

Runx2-P1 and *Supt3h* promoters can physically interact and regulate *Runx2-P1* expression *in-trans*

The increase of *Runx2-P1* and *Supt3h* interaction frequency as well as the enrichment of RUNX2 and presence of DHS at the *Supt3h* promoter, without affecting *Supt3h* expression, suggests that regulation of the *Runx2-P1* promoter includes chromatin alterations that do not affect *Supt3h* gene transcription.

To determine if the *Supt3h* promoter region can regulate the transcriptional activity of the *Runx2-P1* promoter, we generated a reporter construct by cloning a ∼3-kb *Supt3h* fragment (−1154 to +1915 of the *Supt3h* TSS) upstream of a ∼1-kb (−965 to −16) *Runx2-P1* promoter sequence that

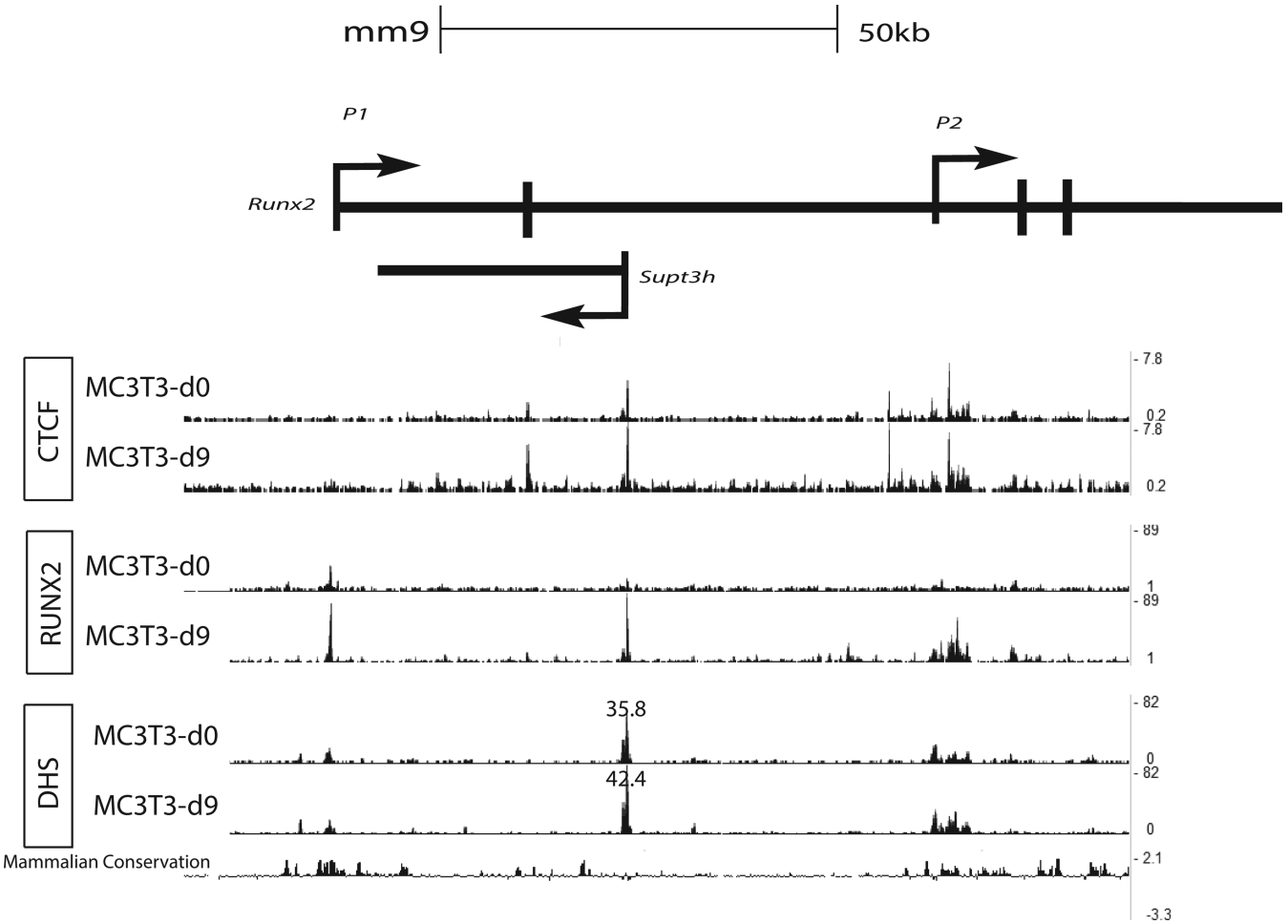

Figure 3. The epigenetic landscape of the *Runx2* locus during differentiation. DNaseI-seq and ChIP-seq signal tracks for CTCF and RUNX2 enrichment in d0 and d9 MC3T3s. The DHS scores for the *Supt3h* promoter region are also shown.

drives the luciferase reporter gene (40). The 3-kb *Supt3h* fragment partially overlaps with the looping BglII fragment (Figure 2a). Luciferase reporter assays were conducted in undifferentiated (d0) and post-differentiated (d6) MC3T3-E1 cultures. We observe that the 3-kb *Supt3h* promoter construct suppresses the transcriptional activity of the *Runx2-P1* promoter in both d0 and d6 cultures (Figure 5a). Similar effects were observed when different fragments within the upstream 2.5 kb of the *Supt3h* promoter were assayed for reporter gene expression (Supplementary Figure S4). Some of the regions tested also include the DNaseI hypersensitive site in Figure 3.

Taking into account the increase in *Runx2-P1* transcription by ∼3-fold in d9 MC3T3 cultures (Figure 4a) accompanied by the increase in looping interaction frequency (Figure 2a), the suppressive effect on luciferase reporter activity of the *Supt3h* promoter was unexpected. We therefore reasoned that the transcriptional effect of *Runx2-P1* we observed with the different *Supt3h* promoter regions might be related to undefined spacing requirements for these regulatory sequences. When these regions are placed in tandem in the same plasmid (*in-cis*), they are in an artificial configuration removed from their endogenous context. Therefore, to better recapitulate the endogenous context, we asked whether *Runx2-P1* and *Supt3h* promoter regions could regulate *Runx2-P1* transcription while residing on different plasmid constructs via an *in-trans* association.

To test whether the *Supt3h* promoter region can physically interact with and regulate the *Runx2-P1* promoter activity *in-trans*, we employed a modified 3C assay that we have named 'i3C' (Figure 5b). In the i3C method, as summarized in Figure 5b, we used the (−965 to −16) *Runx2-P1* promoter pGL3 luciferase construct, and we also cloned the 3.3-kb *Supt3h* promoter region (−1154 to +1915) into a TOPO plasmid to generate the *Supt3h*-TOPO construct.

MC3T3-E1 cultures were co-transfected with the *Runx2-P1* pGL3 luciferase construct along with the *Supt3h*-TOPO construct to test if they associate with each other. Parallel cultures were co-transfected with the *Runx2-P1* pGL3 luciferase construct along with an empty-TOPO plasmid to serve as a negative control, and the empty pGL3 luciferase construct along with the empty-TOPO construct to serve as a normalization control for the i3C experiment. The *Supt3h*–TOPO vector combination was also added as a control. After co-transfection, cells were differentiated for 5 days and treated in the same manner as cultures subjected

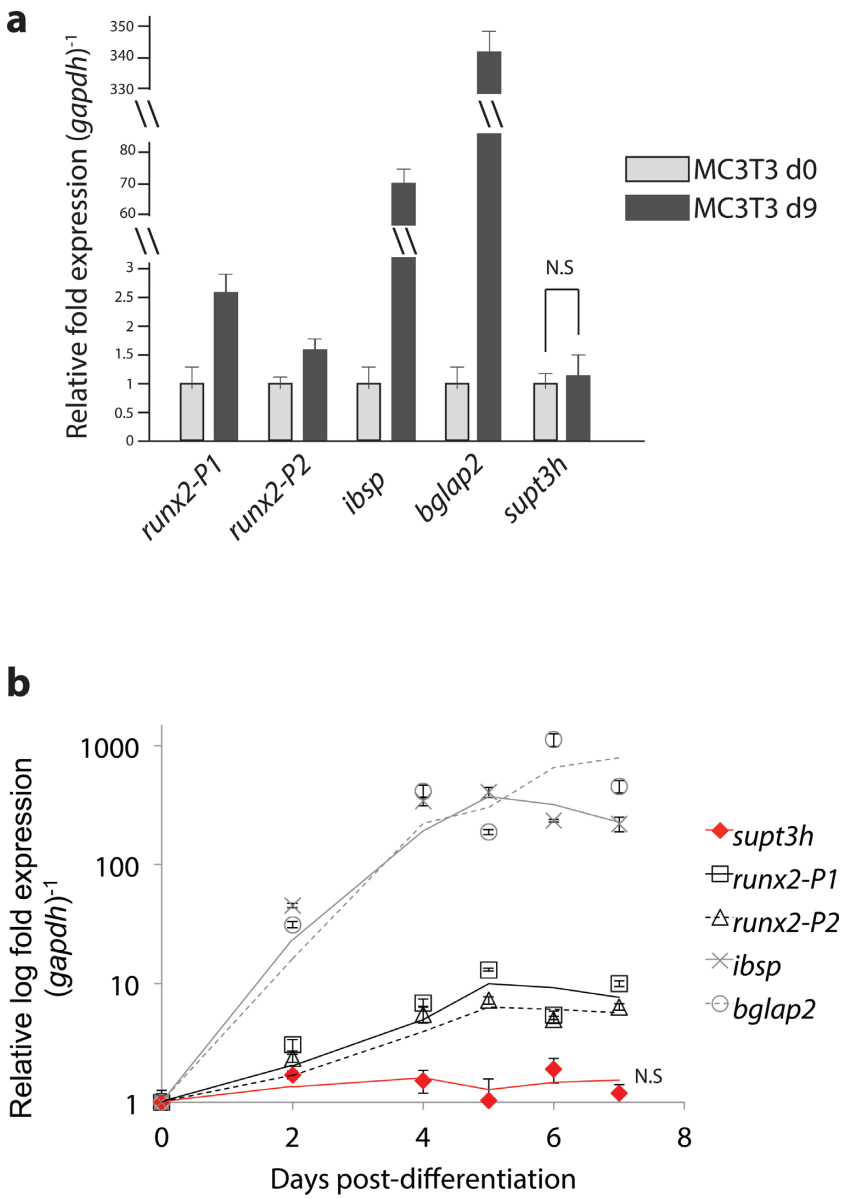

Figure 4. qPCR analysis of bone-specific genes during osteoblast differentiation. (**a**) Relative expression levels of *runx2-P1*, *runx2-P2*, *ibsp*, *bglap2* and *supt3h* in d0 and d9 cultures. Relative expression was normalized to 'd0' values. (**b**) Time course qPCR expression analysis of bone-related genes in d0, d2, d4, d5, d6 and d7. (*$P < 0.05$ by Student's *t*-test).

to the 3C methodology (see the Materials and Methods section). To assess the ligation frequency between the plasmids, PCR quantification was performed with i3C primers specific to either pGL3 or TOPO plasmid backbone sequences.

Our results reveal that when normalized to the empty pGL3 and empty-TOPO co-transfection control, d5 cultures transfected with the *Runx2-P1* pGL3 luciferase and *Supt3h*-TOPO constructs showed a ∼2.5-fold increase in interaction frequency compared to the *Runx2-P1* pGL3 and empty-TOPO constructs (Figure 5c). In other words, pGL3 luciferase and TOPO constructs interact at a higher frequency only when the TOPO construct contains the 3.3-kb *Supt3h* region and the pGL3 constructs the *Runx2-P1* promoter region (Figure 5c, third and fourth lanes). Our i3C results demonstrate that co-transfected plasmids can physically interact. More importantly, we demonstrate that the *Supt3h* and the *Runx2-P1* promoters on separate plasmids can associate *in-trans* outside of their endogenous chromosomal context.

We next tested whether the *Supt3h* promoter region can regulate the activity of the *Runx2-P1* promoter using the *in-trans* system described above. We co-transfected MC3T3 cells with the *Runx2-P1* pGL3 luciferase construct together with either *Supt3h*-TOPO or empty-TOPO constructs. We then assayed for *Runx2-P1* promoter activity via luciferase reporter assay at daily intervals throughout differentiation (d2, d4, d5, d6 and d7) (Figure 5d). Surprisingly, cultures transfected with *Supt3h*-TOPO displayed a nearly 40% increase in luciferase activity at d7 compared to cultures transfected with the empty-TOPO construct (Figure 5d).

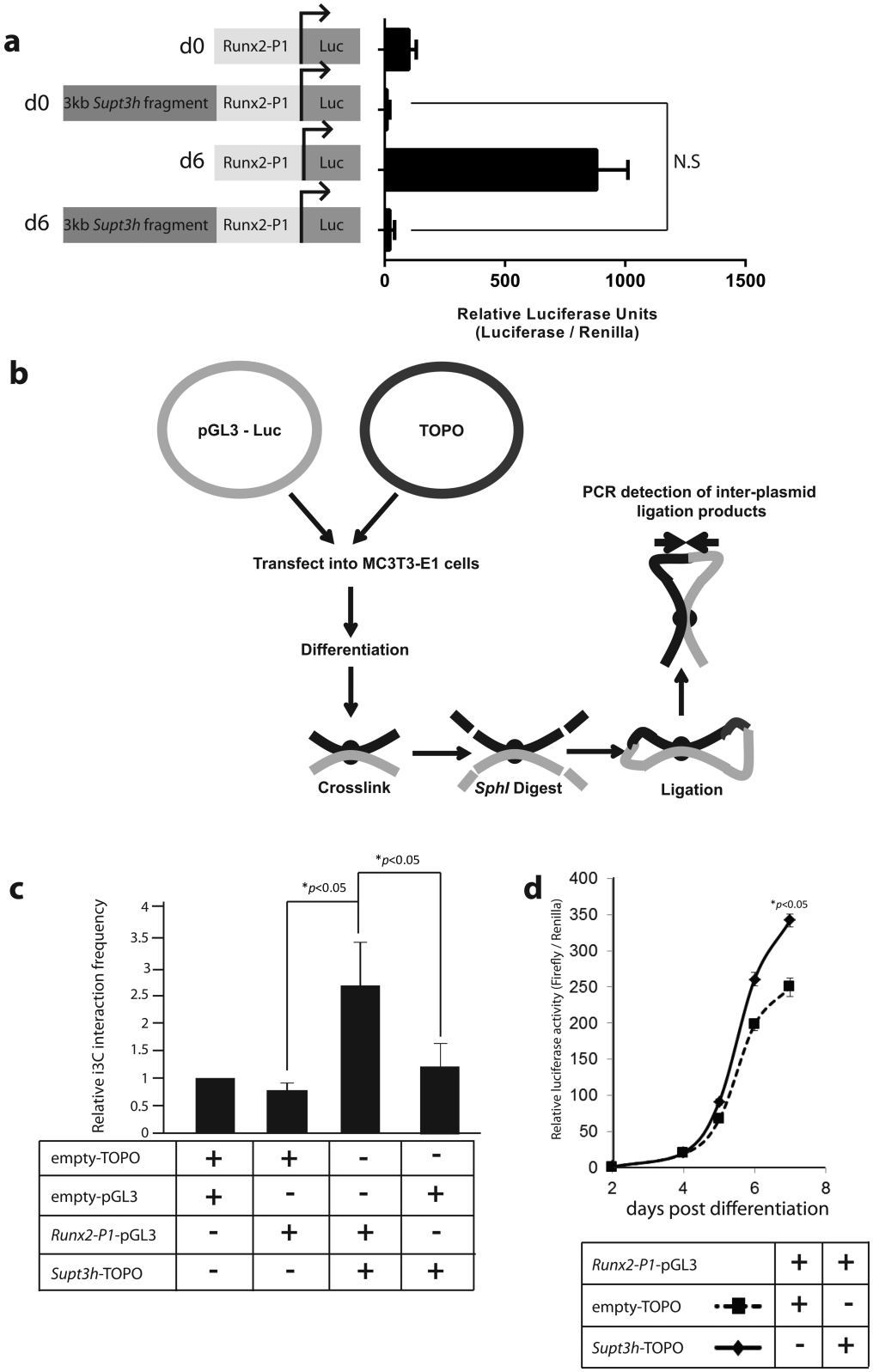

Figure 5. Inter-plasmid 3C and *in-trans* luciferase assay. (**a**) Luciferase reporter assay of the *Supt3h* construct in d0 and d6 MC3T3-E1 cells. (**b**) The schematic of the interplasmid-3C assay. After the co-transfection of pGL3 and TOPO vectors, chromosome conformation capture is performed, and the proximity of two plasmids is assessed via primers designed on the backbone of the vectors. (**c**) i3C analysis of co-transfected plasmids. The y-axis represents the relative ligation frequency between the plasmids. The co-transfection of plasmids was represented with a '+' below. Error bars: S.E.M. (**d**) *In-trans* luciferase assay. Cells were transfected with either *Supt3h*-TOPO or empty-TOPO construct, and relative luciferase activity was measured at indicated time points. (**P* values assessed by Student's *t*-test.)

The increase in *Runx2-P1* promoter activity after d6 suggests that the regulatory sequences within the *Supt3h* promoter, which exerted a suppressive effect *in-cis* (Figure 5a), can positively regulate the *Runx2-P1* promoter activity *in-trans* in a differentiation-dependent manner.

DISCUSSION

Recent mapping of genome-wide chromosomal interactions in both prokaryotes and eukaryotes suggests the regulatory importance of long-range associations to control gene expression (41,42). During development, the genome undergoes drastic structural and regulatory changes resulting in the alteration of cell identity. RUNX2 is an important regulator of bone formation and a key player in metastatic bone disease (1–5). Perturbations to the *Runx2* gene and reduction of its transcript levels result in cleidocranial dysplasia (43). Due to its importance in development and disease, understanding the structure and the regulation of the *Runx2* gene is relevant to many regulatory pathways.

Genetic evidence suggests that mammalian *Runx* genes acquired the utilization of two promoters (*P1* and *P2*) prior to their duplication event (44). Therefore, if a regulatory relationship between different sequences within the *Runx* locus existed before its duplication, it is possible that this relationship may be conserved throughout evolution in paralogue *Runx* genes. In the light of these findings, the syntenic relationship between *Runx2* and *Supt3h* has prompted us to hypothesize that an architectural and regulatory relationship exists between these promoter regions. Apart from the syntenic relationship, the fact that the *Supth3h* promoter is embedded between *Runx2-P1* and *P2* promoters hints at the possibility that the *Supt3h* promoter sequence may have been co-opted by the *Runx2-P1* promoter as an enhancer. Promoters have been shown to act as enhancers for other genes (23).

During *Runx* gene duplication, although the syntenic relationship with *Supt3h* may have been lost, the dependency of an intronic enhancer may have been retained in the *Runx1* and *Runx3* gene loci. Evidence for such conservation of *cis*-regulatory elements is observed in the *Runx1* gene, a paralogue of *Runx2*. *Runx1* has a similar gene structure to *Runx2*, with two isoforms transcribed from two distinct promoters. RUNX1 is required for hematopoietic cell development. Markova *et al.* reported that in human lymphoid and erythroid cell lines, there is a higher-order looping structure between the *Runx1-P1* and an intronic element ∼35 kb downstream of this promoter (45). The distance and the localization of the intronic looping element in the *Runx1* locus coincide with the syntenic *Supt3h* promoter in the *Runx2* locus. This result is consistent with the fact that alternative promoter usage of *Runx* genes existed before their duplication (44), and it suggests the existence of a similar structural relationship in the *Runx2* gene locus.

When we queried the ENCODE database, we found that long-range chromatin interactions exist between *Runx2-P1* and *Supt3h* in human lung fibroblast (IMR90), breast cancer (MCF7) and leukemia (K562) cell lines (Figure 1). Interestingly, although the PolII ChIA-PET data in K562 and MCF7 cells suggested a looping interaction between *Supt3h* and *Runx2* promoters, there was little to undetectable PolII ChIP-seq signal at the *Runx2-P1* promoter (Figure 1). A similar low-level PolII signal is also observed at *Runx2-P1* in IMR90 cells. These data indicate that a basal level of *Supt3h–Runx2-P1* interaction is present regardless of *Runx2-P1* expression.

Synteny results from selective evolutionary pressure. The selective pressure could be related to a requirement for looping events between the *Runx2-P1*, *Runx2-P2* and *Supt3h* promoter regions. These findings not only correlate with the evolutionary relationship and the conservation of this synteny across many organisms, but are also consistent with the idea of a basal structural interaction between these promoters. Further evidence to support this idea comes from the 3C analysis with mouse macrophage RAW 264.7 cells (Figure 1d) and undifferentiated d0 pre-osteoblastic cells (Figure 2a). RAW 264.7 cells have minimal expression of *Runx2-P2* and lack the expression of *Runx2-P1* isoforms (Supplementary Figure S2), and d0 MC3T3 cells show low levels of *Runx2-P1* activity (Figure 4a). However, we were able to observe an interaction between the *Supt3h* and *Runx2-P1* promoters in these cells. Moreover, we also detected a structural link between the *Runx2-P1* and *Runx2-P2* promoters (Figure 2b), a phenomenon also observed in the *P1* and *P2* promoters of the *Runx1* gene locus (45).

Another interesting finding is that the *Supt3h* promoter region is epigenetically altered during differentiation, as indicated by the increase in DHS and the increase of CTCF and RUNX2 enrichment (Figure 3). However, *Supt3h* expression levels remain unchanged throughout this process. The interaction frequency between the *Runx2-P1* and *Supt3h* promoters exhibits a striking increase during osteoblastic differentiation (Figure 2a). When the 3C anchor is positioned on the *Runx2-P2* promoter, the data also suggest that three promoters (*Runx2-P1*, *Runx2-P2* and *Supt3h*) are in close proximity in d9 MC3T3 cultures (Figure 2b), a phenomenon also seen to occur in K562 cells as assessed by the PolII ChIA-PET data (data not shown). Taken together, our observations suggest that local changes occurring at the *Supt3h* promoter act by modulating *Runx2-P1* activity. Alternatively, the increase of CTCF enrichment may reflect the presence of an activated insulator element that flanks the *Supt3h* promoter region during differentiation. The recruitment of CTCF to the *Supt3h* promoter region may also act to prevent the regulatory action of upstream sequences that may interfere with *Supt3h* transcription. Moreover, at d0, RUNX2 binds primarily to *P2*, but not to the *P1* promoter. The RUNX2 protein is known to interact and co-bind to DNA with several other co-factors such as C/EBPβ (38,46,47). It is possible that differential binding of co-factors to RUNX2 may change its affinity for its binding sites. Additionally, the *Runx2-P1* promoter contains binding sites for C/EBPβ, OCT1, AP-1, RUNX2, MSX2/DLX3/DLX5, ATF, HLH/TWIST, VDRE, LEF/TCF, NKX, NF-1, SP1 and ETS. Combinatorial binding of these factors may also play roles in selectively recruiting RUNX2 to these promoters.

We also demonstrate that the interaction between the *Runx2-P1* and *Supt3h* promoters impacts the activity of the *Runx2-P1* promoter. We chose to include the −965/−16 region of the *Runx2-P1* promoter, as this region has been shown to adequately respond to differentiation conditions

(40). Also, there are three RUNX binding sites within the 5′ UTR of the *Runx2-P1* promoter centered at +31, +39 and +49 bp downstream of the *Runx2-P1* TSS. These RUNX motifs have been shown to suppress *Runx2* expression as part of a negative feedback loop (30). Luciferase reporter assays with different *Supt3h* constructs cloned *in-cis* upstream of the *Runx2-P1* promoter driving luciferase showed a reduction of *Runx2-P1* activity (Figure 5a). Because the *Supt3h* and *Runx2-P1* promoter regions reside more than 35 kb away from each other in their endogenous context, we hypothesized that testing these regions in a '*trans*' configuration would better recapitulate the regulation occurring in the endogenous setting. We therefore measured the effect of the *Supt3h* promoter on the *Runx2-P1* promoter while on separate plasmids. Although the ability for regulatory regions residing on separate plasmid constructs to modulate activity *in-trans* has been demonstrated previously (48,49), the majority of *in vitro* assays that test for enhancer–promoter interactions are performed within the same DNA construct, *in cis,* where the enhancer is cloned 5′ to the promoter. Functional assays aimed to validate long-range, *cis*-acting interactions are also performed in this manner. To test our hypothesis that the *Supt3h* promoter could interact with *Runx2-P1* when introduced on separate plasmids, we utilized a modified 3C protocol that we termed 'i3C' (Figure 5b). i3C results show that there is a ∼2.5-fold higher interaction frequency between plasmids containing the *Runx2-P1* and *Supt3h* sequences than control plasmids (Figure 5c). This result indicates that regulatory sequences of the *Supt3h* promoter need to be at a distance from the *Runx2-P1* promoter. Under these same conditions, when *Runx2-P1* promoter driven luciferase activity was assayed throughout differentiation, a significant increase is observed (Figure 5d) when co-transfected with the *Supt3h*-TOPO construct but not the empty-TOPO construct, suggesting a differentiation-dependent activator role of the *Supt3h* promoter.

It is still not clear why background levels of structural interactions between these two promoters exist in cells that lack *Runx2-P1* transcription. However, we have shown a bone-differentiation-specific regulatory function of the *Supt3h* promoter region on *Runx2-P1* promoter driven transcription. It is important to point out that in our 3C analysis, we only queried a ∼±300-kb genomic region surrounding the *Runx2* locus (Figure 2a). Other studies have indicated that enhancers can exert their functions from hundreds, or even thousands, of kilobases away (32). It may be that additional distant regulatory regions that are located outside the ∼600-kb *Runx2* locus become associated with the *Runx2-P1* promoter region and contribute to its regulation.

Taken together, our results demonstrate a novel aspect of *Runx2* gene structure and regulation. We also demonstrate a role for *Supt3h* association with the *Runx2-P1* promoter in modulating the bone-specific activity of the *Runx2-P1* promoter. Further experiments such as deletion of the *Supt3h* promoter region will be needed to provide additional insight into the transcriptional control of the *Runx2*-P1 promoter during osteogenesis.

SUPPLEMENTARY DATA

Supplementary Data are available at NAR Online.

ACKNOWLEDGMENTS

We thank the Stein and Imbalzano lab members for stimulating discussions, Bryan Lajoie for technical help with the 3C primer design, and Jennifer Díaz for administrative assistance.

ACCESSION NUMBER

The DNase-seq data were deposited under the accession GSE55046 in ENCODE.

FUNDING

National Institutes of Health [P01 AR048818 to G.S.S., P01 CA082834 to G.S.S., R01 AR039588 to G.S.S. and J.B.L., R01 GM56244 to A.N.I.]. Funding for open access charge: NIH [P01 AR048818, P01 CA082834, R01 AR039588].
Conflict of interest statement. None declared.

REFERENCES

1. Stein, G.S., Lian, J.B., van Wijnen, A.J., Stein, J.L., Montecino, M., Javed, A., Zaidi, S.K., Young, D.W., Choi, J.Y., and Pockwinse, S.M. Stein, G.S., Lian, J.B., van Wijnen, A.J., Stein, J.L., Montecino, M., Javed, A., Zaidi, S.K., Young, D.W., Choi, J.Y., and Pockwinse, S.M. (2004) Runx2 control of organization, assembly and activity of the regulatory machinery for skeletal gene expression. *Oncogene*, **23**, 4315–4329.
2. Otto, F., Thornell, A.P., Crompton, T., Denzel, A., Gilmour, K.C., Rosewell, I.R., Stamp, G.W., Beddington, R.S., Mundlos, S., and Olsen, B.R. *et al.*Otto, F., Thornell, A.P., Crompton, T., Denzel, A., Gilmour, K.C., Rosewell, I.R., Stamp, G.W., Beddington, R.S., Mundlos, S., and Olsen, B.R. (1997) Cbfa1, a candidate gene for cleidocranial dysplasia syndrome, is essential for osteoblast differentiation and bone development. *Cell*, **89**, 765–771.
3. Komori, T., Yagi, H., Nomura, S., Yamaguchi, A., Sasaki, K., Deguchi, K., Shimizu, Y., Bronson, R.T., Gao, Y.H., and Inada, M. *et al.*Komori, T., Yagi, H., Nomura, S., Yamaguchi, A., Sasaki, K., Deguchi, K., Shimizu, Y., Bronson, R.T., Gao, Y.H., and Inada, M. (1997) Targeted disruption of Cbfa1 results in a complete lack of bone formation owing to maturational arrest of osteoblasts. *Cell*, **89**, 755–764.
4. Ducy, P., Zhang, R., Geoffroy, V., Ridall, A.L., and Karsenty, G.Ducy, P., Zhang, R., Geoffroy, V., Ridall, A.L., and Karsenty, G. (1997) Osf2/Cbfa1: a transcriptional activator of osteoblast differentiation. *Cell*, **89**, 747–754.
5. Ducy, P., Starbuck, M., Priemel, M., Shen, J., Pinero, G., Geoffroy, V., Amling, M., and Karsenty, G.Ducy, P., Starbuck, M., Priemel, M., Shen, J., Pinero, G., Geoffroy, V., Amling, M., and Karsenty, G. (1999) A Cbfa1-dependent genetic pathway controls bone formation beyond embryonic development. *Genes Dev.*, **13**, 1025–1036.
6. Lou, Y., Javed, A., Hussain, S., Colby, J., Frederick, D., Pratap, J., Xie, R., Gaur, T., van Wijnen, A.J., and Jones, S.N. *et al.*Lou, Y., Javed, A., Hussain, S., Colby, J., Frederick, D., Pratap, J., Xie, R., Gaur, T., van Wijnen, A.J., and Jones, S.N. (2009) A Runx2 threshold for the cleidocranial dysplasia phenotype. *Hum. Mol. Genet.*, **18**, 556–568.
7. Choi, J.Y., Pratap, J., Javed, A., Zaidi, S.K., Xing, L., Balint, E., Dalamangas, S., Boyce, B., van Wijnen, A.J., and Lian, J.B. *et al.*Choi, J.Y., Pratap, J., Javed, A., Zaidi, S.K., Xing, L., Balint, E., Dalamangas, S., Boyce, B., van Wijnen, A.J., and Lian, J.B. (2001) Subnuclear targeting of Runx/Cbfa/AML factors is essential for tissue-specific differentiation during embryonic development. *Proc. Natl. Acad. Sci. U.S.A.*, **98**, 8650–8655.

8. Zaidi, S.K., Young, D.W., Montecino, M.A., Lian, J.B., van Wijnen, A.J., Stein, J.L., and Stein, G.S.Zaidi, S.K., Young, D.W., Montecino, M.A., Lian, J.B., van Wijnen, A.J., Stein, J.L., and Stein, G.S. (2010) Mitotic bookmarking of genes: a novel dimension to epigenetic control. *Nat. Rev. Genet.*, **11**, 583–589.
9. Pockwinse, S.M., Kota, K.P., Quaresma, A.J., Imbalzano, A.N., Lian, J.B., van Wijnen, A.J., Stein, J.L., Stein, G.S., and Nickerson, J.A.Pockwinse, S.M., Kota, K.P., Quaresma, A.J., Imbalzano, A.N., Lian, J.B., van Wijnen, A.J., Stein, J.L., Stein, G.S., and Nickerson, J.A. (2011) Live cell imaging of the cancer-related transcription factor RUNX2 during mitotic progression. *J. Cell. Physiol.*, **226**, 1383–1389.
10. Ali, S.A., Dobson, J.R., Lian, J.B., Stein, J.L., van Wijnen, A.J., Zaidi, S.K., and Stein, G.S. Ali, S.A., Dobson, J.R., Lian, J.B., Stein, J.L., van Wijnen, A.J., Zaidi, S.K., and Stein, G.S. (2012) A RUNX2-HDAC1 co-repressor complex regulates rRNA gene expression by modulating UBF acetylation. *J. Cell Sci.*, **125**, 2732–2739.
11. Harada, H., Tagashira, S., Fujiwara, M., Ogawa, S., Katsumata, T., Yamaguchi, A., Komori, T., and Nakatsuka, M.Harada, H., Tagashira, S., Fujiwara, M., Ogawa, S., Katsumata, T., Yamaguchi, A., Komori, T., and Nakatsuka, M. (1999) Cbfa1 isoforms exert functional differences in osteoblast differentiation. *J. Biol. Chem.*, **274**, 6972–6978.
12. Liu, J.C., Lengner, C.J., Gaur, T., Lou, Y., Hussain, S., Jones, M.D., Borodic, B., Colby, J.L., Steinman, H.A., and van Wijnen, A.J. *et al.*Liu, J.C., Lengner, C.J., Gaur, T., Lou, Y., Hussain, S., Jones, M.D., Borodic, B., Colby, J.L., Steinman, H.A., and van Wijnen, A.J. (2011) Runx2 protein expression utilizes the Runx2 P1 promoter to establish osteoprogenitor cell number for normal bone formation. *J. Biol. Chem.*, **286**, 30057–30070.
13. Yu, J., Madison, J.M., Mundlos, S., Winston, F., and Olsen, B.R.Yu, J., Madison, J.M., Mundlos, S., Winston, F., and Olsen, B.R. (1998) Characterization of a human homologue of the Saccharomyces cerevisiae transcription factor spt3 (SUPT3H). *Genomics*, **53**, 90–96.
14. Martinez, E., Kundu, T.K., Fu, J., and Roeder, R.G.Martinez, E., Kundu, T.K., Fu, J., and Roeder, R.G. (1998) A human SPT3-TAFII31-GCN5-L acetylase complex distinct from transcription factor IID. *J. Biol. Chem.*, **273**, 23781–23785.
15. Liu, X., Vorontchikhina, M., Wang, Y.L., Faiola, F., and Martinez, E.Liu, X., Vorontchikhina, M., Wang, Y.L., Faiola, F., and Martinez, E. (2008) STAGA recruits Mediator to the MYC oncoprotein to stimulate transcription and cell proliferation. *Mol. Cell. Biol.*, **28**, 108–121.
16. Barbaric, S., Reinke, H., and Horz, W.Barbaric, S., Reinke, H., and Horz, W. (2003) Multiple mechanistically distinct functions of SAGA at the PHO5 promoter. *Mol. Cell. Biol.*, **23**, 3468–3476.
17. Robertson, A.J., Larroux, C., Degnan, B.M., and Coffman, J.A.Robertson, A.J., Larroux, C., Degnan, B.M., and Coffman, J.A. (2009) The evolution of Runx genes II. The C-terminal Groucho recruitment motif is present in both eumetazoans and homoscleromorphs but absent in a haplosclerid demosponge. *BMC Res. Notes*, **2**, 59.
18. Navratilova, P. and Becker, T.S.Navratilova, P. and Becker, T.S. (2009) Genomic regulatory blocks in vertebrates and implications in human disease. *Brief. Funct. Genomic Proteomic*, **8**, 333–342.
19. Kikuta, H., Laplante, M., Navratilova, P., Komisarczuk, A.Z., Engstrom, P.G., Fredman, D., Akalin, A., Caccamo, M., Sealy, I., and Howe, K. *et al.*Kikuta, H., Laplante, M., Navratilova, P., Komisarczuk, A.Z., Engstrom, P.G., Fredman, D., Akalin, A., Caccamo, M., Sealy, I., and Howe, K. (2007) Genomic regulatory blocks encompass multiple neighboring genes and maintain conserved synteny in vertebrates. *Genome Res.*, **17**, 545–555.
20. Zhou, X., Lowdon, R.F., Li, D., Lawson, H.A., Madden, P.A., Costello, J.F., and Wang, T.Zhou, X., Lowdon, R.F., Li, D., Lawson, H.A., Madden, P.A., Costello, J.F., and Wang, T. (2013) Exploring long-range genome interactions using the WashU Epigenome Browser. *Nat. Methods*, **10**, 375–376.
21. Kent, W.J., Sugnet, C.W., Furey, T.S., Roskin, K.M., Pringle, T.H., Zahler, A.M., and Haussler, D.Kent, W.J., Sugnet, C.W., Furey, T.S., Roskin, K.M., Pringle, T.H., Zahler, A.M., and Haussler, D. (2002) The human genome browser at UCSC. *Genome Res.*, **12**, 996–1006.
22. Dixon, J.R., Selvaraj, S., Yue, F., Kim, A., Li, Y., Shen, Y., Hu, M., Liu, J.S., and Ren, B.Dixon, J.R., Selvaraj, S., Yue, F., Kim, A., Li, Y., Shen, Y., Hu, M., Liu, J.S., and Ren, B. (2012) Topological domains in mammalian genomes identified by analysis of chromatin interactions. *Nature*, **485**, 376–380.
23. Li, G., Ruan, X., Auerbach, R.K., Sandhu, K.S., Zheng, M., Wang, P., Poh, H.M., Goh, Y., Lim, J., and Zhang, J. *et al.*Li, G., Ruan, X., Auerbach, R.K., Sandhu, K.S., Zheng, M., Wang, P., Poh, H.M., Goh, Y., Lim, J., and Zhang, J. (2012) Extensive promoter-centered chromatin interactions provide a topological basis for transcription regulation. *Cell*, **148**, 84–98.
24. Wang, D., Christensen, K., Chawla, K., Xiao, G., Krebsbach, P.H., and Franceschi, R.T.Wang, D., Christensen, K., Chawla, K., Xiao, G., Krebsbach, P.H., and Franceschi, R.T. (1999) Isolation and characterization of MC3T3-E1 preosteoblast subclones with distinct in vitro and in vivo differentiation/mineralization potential. *J. Bone Miner. Res.*, **14**, 893–903.
25. Naumova, N., Smith, E.M., Zhan, Y., and Dekker, J.Naumova, N., Smith, E.M., Zhan, Y., and Dekker, J. (2012) Analysis of long-range chromatin interactions using Chromosome Conformation Capture. *Methods*, **58**, 192–203.
26. Dekker, J., Rippe, K., Dekker, M., and Kleckner, N.Dekker, J., Rippe, K., Dekker, M., and Kleckner, N. (2002) Capturing chromosome conformation. *Science*, **295**, 1306–1311.
27. Kagey, M.H., Newman, J.J., Bilodeau, S., Zhan, Y., Orlando, D.A., van Berkum, N.L., Ebmeier, C.C., Goossens, J., Rahl, P.B., and Levine, S.S. *et al.*Kagey, M.H., Newman, J.J., Bilodeau, S., Zhan, Y., Orlando, D.A., van Berkum, N.L., Ebmeier, C.C., Goossens, J., Rahl, P.B., and Levine, S.S. (2010) Mediator and cohesin connect gene expression and chromatin architecture. *Nature*, **467**, 430–435.
28. Song, L. and Crawford, G.E.**2010**Song, L. and Crawford, G.E. (2010) DNase-seq: a high-resolution technique for mapping active gene regulatory elements across the genome from mammalian cells. *Cold Spring Harb. Protoc.*, pdb.prot5384.
29. Boyle, A.P., Guinney, J., Crawford, G.E., and Furey, T.S.Boyle, A.P., Guinney, J., Crawford, G.E., and Furey, T.S. (2008) F-Seq: a feature density estimator for high-throughput sequence tags. *Bioinformatics*, **24**, 2537–2538.
30. Drissi, H., Luc, Q., Shakoori, R., Chuva De Sousa Lopes, S., Choi, J.Y., Terry, A., Hu, M., Jones, S., Neil, J.C., and Lian, J.B. *et al.*Drissi, H., Luc, Q., Shakoori, R., Chuva De Sousa Lopes, S., Choi, J.Y., Terry, A., Hu, M., Jones, S., Neil, J.C., and Lian, J.B. (2000) Transcriptional autoregulation of the bone related CBFA1/RUNX2 gene. *J. Cell. Physiol.*, **184**, 341–350.
31. Hagege, H., Klous, P., Braem, C., Splinter, E., Dekker, J., Cathala, G., de Laat, W., and Forne, T.Hagege, H., Klous, P., Braem, C., Splinter, E., Dekker, J., Cathala, G., de Laat, W., and Forne, T. (2007) Quantitative analysis of chromosome conformation capture assays (3C-qPCR). *Nat. Protoc.*, **2**, 1722–1733.
32. Sanyal, A., Lajoie, B.R., Jain, G., and Dekker, J.Sanyal, A., Lajoie, B.R., Jain, G., and Dekker, J. (2012) The long-range interaction landscape of gene promoters. *Nature*, **489**, 109–113.
33. Lieberman-Aiden, E., van Berkum, N.L., Williams, L., Imakaev, M., Ragoczy, T., Telling, A., Amit, I., Lajoie, B.R., Sabo, P.J., and Dorschner, M.O. *et al.*Lieberman-Aiden, E., van Berkum, N.L., Williams, L., Imakaev, M., Ragoczy, T., Telling, A., Amit, I., Lajoie, B.R., Sabo, P.J., and Dorschner, M.O. (2009) Comprehensive mapping of long-range interactions reveals folding principles of the human genome. *Science*, **326**, 289–293.
34. Fullwood, M.J., Liu, M.H., Pan, Y.F., Liu, J., Xu, H., Mohamed, Y.B., Orlov, Y.L., Velkov, S., Ho, A., and Mei, P.H. *et al.*Fullwood, M.J., Liu, M.H., Pan, Y.F., Liu, J., Xu, H., Mohamed, Y.B., Orlov, Y.L., Velkov, S., Ho, A., and Mei, P.H. (2009) An oestrogen-receptor-alpha-bound human chromatin interactome. *Nature*, **462**, 58–64.
35. Phillips-Cremins, J.E., Sauria, M.E., Sanyal, A., Gerasimova, T.I., Lajoie, B.R., Bell, J.S., Ong, C.T., Hookway, T.A., Guo, C., and Sun, Y. *et al.*Phillips-Cremins, J.E., Sauria, M.E., Sanyal, A., Gerasimova, T.I., Lajoie, B.R., Bell, J.S., Ong, C.T., Hookway, T.A., Guo, C., and Sun, Y. (2013) Architectural protein subclasses shape 3D organization of genomes during lineage commitment. *Cell*, **153**, 1281–1295.
36. Park, M.H., Shin, H.I., Choi, J.Y., Nam, S.H., Kim, Y.J., Kim, H.J., and Ryoo, H.M.Park, M.H., Shin, H.I., Choi, J.Y., Nam, S.H., Kim, Y.J., Kim, H.J., and Ryoo, H.M. (2001) Differential expression patterns of Runx2 isoforms in cranial suture morphogenesis. *J. Bone Miner. Res.*, **16**, 885–892.

37. Lian, J.B., Javed, A., Zaidi, S.K., Lengner, C., Montecino, M., van Wijnen, A.J., Stein, J.L., and Stein, G.S.Lian, J.B., Javed, A., Zaidi, S.K., Lengner, C., Montecino, M., van Wijnen, A.J., Stein, J.L., and Stein, G.S. (2004) Regulatory controls for osteoblast growth and differentiation: role of Runx/Cbfa/AML factors. *Crit. Rev. Eukaryot. Gene Expr.*, **14**, 1–41.
38. Wu, H., Whitfield, T.W., Gordon, J.A., Dobson, J.R., Tai, P.W., van Wijnen, A.J., Stein, J.L., Stein, G.S., and Lian, J.B.Wu, H., Whitfield, T.W., Gordon, J.A., Dobson, J.R., Tai, P.W., van Wijnen, A.J., Stein, J.L., Stein, G.S., and Lian, J.B. (2014) Genomic occupancy of Runx2 with global expression profiling identifies a novel dimension to control of osteoblastogenesis. *Genome Biol.*, **15**, R52.
39. Quarles, L.D., Yohay, D.A., Lever, L.W., Caton, R., and Wenstrup, R.J.Quarles, L.D., Yohay, D.A., Lever, L.W., Caton, R., and Wenstrup, R.J. (1992) Distinct proliferative and differentiated stages of murine MC3T3-E1 cells in culture: an in vitro model of osteoblast development. *J. Bone Miner. Res.*, **7**, 683–692.
40. Tai, P.W., Wu, H., Gordon, J.A., Whitfield, T.W., Barutcu, A.R., van Wijnen, A.J., Lian, J.B., Stein, G.S., and Stein, J.L.doi: 10.1016/j.gene.2014.05.044Tai, P.W., Wu, H., Gordon, J.A., Whitfield, T.W., Barutcu, A.R., van Wijnen, A.J., Lian, J.B., Stein, G.S., and Stein, J.L. (2014) Gene,.
41. Le, T.B., Imakaev, M.V., Mirny, L.A., and Laub, M.T.Le, T.B., Imakaev, M.V., Mirny, L.A., and Laub, M.T. (2013) High-resolution mapping of the spatial organization of a bacterial chromosome. *Science*, **342**, 731–734.
42. Jin, F., Li, Y., Dixon, J.R., Selvaraj, S., Ye, Z., Lee, A.Y., Yen, C.A., Schmitt, A.D., Espinoza, C.A., and Ren, B.Jin, F., Li, Y., Dixon, J.R., Selvaraj, S., Ye, Z., Lee, A.Y., Yen, C.A., Schmitt, A.D., Espinoza, C.A., and Ren, B. (2013) A high-resolution map of the three-dimensional chromatin interactome in human cells. *Nature*, **503**, 290–294.
43. Mundlos, S., Otto, F., Mundlos, C., Mulliken, J.B., Aylsworth, A.S., Albright, S., Lindhout, D., Cole, W.G., Henn, W., and Knoll, J.H. *et al.*Mundlos, S., Otto, F., Mundlos, C., Mulliken, J.B., Aylsworth, A.S., Albright, S., Lindhout, D., Cole, W.G., Henn, W., and Knoll, J.H. (1997) Mutations involving the transcription factor CBFA1 cause cleidocranial dysplasia. *Cell*, **89**, 773–779.
44. Rennert, J., Coffman, J.A., Mushegian, A.R., and Robertson, A.J.Rennert, J., Coffman, J.A., Mushegian, A.R., and Robertson, A.J. (2003) The evolution of Runx genes I. A comparative study of sequences from phylogenetically diverse model organisms. *BMC Evol. Biol.*, **3**, 4.
45. Markova, E.N., Kantidze, O.L., and Razin, S.V.Markova, E.N., Kantidze, O.L., and Razin, S.V. (2011) Transcriptional regulation and spatial organisation of the human AML1/RUNX1 gene. *J. Cell. Biochem.*, **112**, 1997–2005.
46. Li, X., Decker, M., and Westendorf, J.J.Li, X., Decker, M., and Westendorf, J.J. (2010) TEThered to Runx: novel binding partners for runx factors. *Blood Cells Mol. Dis.*, **45**, 82–85.
47. Meyer, M.B., Benkusky, N.A., and Pike, J.W.Meyer, M.B., Benkusky, N.A., and Pike, J.W. (2014) The RUNX2 cistrome in osteoblasts: characterization, downregulation following differentiation and relationship to gene expression. *J. Biol. Chem.*, **289**, 16016–16031.
48. Zullo, J.M., Demarco, I.A., Pique-Regi, R., Gaffney, D.J., Epstein, C.B., Spooner, C.J., Luperchio, T.R., Bernstein, B.E., Pritchard, J.K., and Reddy, K.L. *et al.*Zullo, J.M., Demarco, I.A., Pique-Regi, R., Gaffney, D.J., Epstein, C.B., Spooner, C.J., Luperchio, T.R., Bernstein, B.E., Pritchard, J.K., and Reddy, K.L. (2012) DNA sequence-dependent compartmentalization and silencing of chromatin at the nuclear lamina. *Cell*, **149**, 1474–1487.
49. Xu, M. and Cook, P.R.Xu, M. and Cook, P.R. (2008) Similar active genes cluster in specialized transcription factories. *J. Cell Biol.*, **181**, 615–623.